Frontiers + Innovation
2009 CSPG CSEG CWLS CONVENTION • CALGARY, ALBERTA, CANADA

Regime Rays: Visualizing the Fermat/Snell Loci in Homogeneous Anisotropic Media

William J. Vetter, P.Eng. (NF), Ph.D., (ret. Prof. Eng., Memorial U., NF Canada)
vetterb@sympatico.ca   Kitchener, ON

Summary

Present understanding and analytical encapsulation of anisotropy kinematics, even in homogeneous anisotropy medium segments which are here the focus, is incomplete/incorrect re the familiar Fermat/Snell ray theory premises [-> *FS-rays*]. The traveltime expression $t_{ON} = t_{OE} = (r_E \bullet n_N)/\ v_N\ (n_N\ ,\ \ c_{i\ j},\ \rho)$, attributed to Green (Love 1927, Rudzki 1911), has been deemed essentially a mode-specific plane-wave progression dictate [here $_{O}$, $_{N}$, $_{E}$ subcripts designate Origin, front-Normal points/directions, Energy-flux arrival- points/directions]. It is moreso a constraint, call it an *ansatz* (starting premise), which for particular homogeneous anisotropic medium models and specified front-normal direction firms direction/progression-speed of *FS-ray* segmentals in part along front-normal direction but, it turns out, with complementing segmentals with maximally two other orientations. *Regime rays* is label for representation loci, when like-oriented segmentals have been re-ordered to single segments, and those segments are then linked.

Through *regime rays* we can discern and quantify significant analytical *FS-rays* detail, the time-fractions and segment lengths plus progression speeds for the three or fewer oriented segments. Those details yield the significant *FS-ray*-specific characterizing velocities for the along-paths velocity distributions $\{v_{APPARENT}$, $v_{TIME\text{-}AVE}$, v_{RMS}, $v_{PATH\text{-}MEAN}\}$; also l_{PATH} which are true pathlengths for intangible *FS-ray* loci.

All this comes from overlooked extra prescribed directions/progression-speeds detail in sequenced mode-relevant eikonal equations, relevant for *FS-rays* for given front-normal directions. The *FS-rays* per se, say in medium natural coordinate frame, progressing mode-specific from point-shots $\boldsymbol{r_O}$ at origin to $\boldsymbol{r_E}$-front-points, are anchored to their energy flux line-loci, the ‘so-called *group*- or *ray*-velocity representation loci’. Beyond analytical essentials previously communicated I provide here simulations/ visualization for all modes of an orthorhombic standard model. *Regime rays* clarify the long-puzzling detail between paired points on the wave surfaces and their *ansatz*-front-normal velocity representation surfaces.

From traveltime *ansatz* to *regime rays* models

It is well established that wave propagation disturbances through composites of fine-structured layering and fine-structured heterogeneities broadly, have EMT (effective medium theory, long wavelength regime) progression speeds that are virtually constant beyond a distinct transition zone re wavelength/composites-repetition-thickness ratio (e.g. Macbeth 2002). I suggest that Fermat’s principle and Snell’s law should apply in such composites also for long wavelength regime *FS-rays*, for progression directions not just orthogonal or parallel to ordered layering or other fine-scale structured heterogeneity. This can be credibly expected, because in the broader physics context Snell’s law and Fermat’s principle are encompassed within the remarkable ‘*principle of least action*’ of Maupertuis [1746], [also Leibniz, Euler, Hamilton, Feynman,…]. At any rate, what manifests from this hypothesis agrees with analytical models and kinematics manifestations in diverse experiments. As simplest example take the above pathtime *ansatz*

t_{ON} = t_{OE} = ($\boldsymbol{r_E} \bullet \boldsymbol{n_N}$)/ v_N ($\boldsymbol{n_N}$, $c_{i\,j}$,ρ), but reduced to progression paths in just the x.vs.z plane as $t_{ON} = t_{OE}$ = ($x_E \sin\theta$ + $z_E \cos\theta$) / v_N , with θ as polar angle re z-axis direction. Then if $x_E > z_E \tan\theta$, the as two segments partitioned equivalent is $t_{ON} = t_{OE}$ = (z_E /$cos\theta$)/ v_N + (x - z_E $tan\theta$)/(v_N /$sin\theta$). First segment has length $l_1 = (z_E /cos\theta)$ with progression speed $v_1 = v_N$, and the second $l_2 = (x - z_E\ tan\theta)$ with speed $v_2 = (v_N /sin\theta) > v_N$. Transition $v_1 = v_N$ to $v_2 = v_N /sin\theta$ conforms with Snell's law, front-normal oriented l_1 of *regime ray* in y=0 plane refracting into x-direction oriented l_2 , ending at front point [x_E z_E].

Else if $z_E \tan\theta > x_E$, the *ansatz* transforms to $t_{ON} = t_{OE}$ = (x_E /$sin\theta$)/ v_N + (z_E –x_E / $tan\theta$)/(v_N /$cos\theta$), with $l_1 = (x_E /sin\theta)$ and speed $v_1 = v_N$ front-normal oriented. Then Snell's law conforming refraction produces z-directed $l_2 = (z_E - x_E / tan\theta)$ with $v_2 = (v_N /cos\theta) > v_N$, ending at [x_E z_E] front-point.

The common pathtime *ansatz* expression has been reframed in two ways, depending on specific association detail between front-normal orientations and for given medium parameters consequent energy flux loci (so-called ray- or group-velocity representation loci), both with two-segmented *regime ray* components.

The general *ansatz* can/must be elaborated to one of 18 different expanded detail forms [really 25, of which 7 have single-direction loci]. *Regime rays* are analytical representations for the significant *FS-rays* detail, through aggregation of same-oriented segmentals to single segments. The *regime rays* condense unknown detail re sequenced segmentals into analytical expressions which reveal then essence of that detail. Much of that analytical detail is can be found in a previous Abstract (Vetter 2007, accessible through CSEG: '2007 CSPG CSEG Joint Convention', Seismic Processing II).

Orthorhombic Medium Simulation Example

Figures 1 to 3 below show *regime rays* simulation detail for Schoenberg and Helbig's (1997)'orthorhombic standard model'. I have used Helbig's explicit Kelvin-Christoffel matrix expansion (1994, Appendix 4B, short version valid for orthorhombic and higher symmetry in medium natural coordinate frame), and a novel compact expression for vectored $\boldsymbol{r}_E$, derived from the pathtime *ansatz* [(eqn 1b) in spherical coordinates (θ, ϕ)], together with the pathtime minimizing derivatives re (θ, ϕ). The below equation 2 is its column-vectored form, after re-converting from spherical- back to rectangular coordinates.

As an important 'aside', eqn.2, columned as shown, is variously incorrect in the literature [e.g. Helbig 1994, p.13 eqn.1a.6{without common dispersion term}; Mensch and Rasolofosaon 1997 eqn.12; ...]. Further, Auld's (1973) suggested 'carrier modulation' analogy, [velocity of carrier<--> vectored *phase velocity*, velocity of modulation envelop<-->vectored *group*- or *ray*- *velocity*] is not realistic/ applicable, nor are then '*phase*-' and '*group-velocity*' really relevant or proper designations for context of the *FS-ray*s *ansatz*.

Equation (3), also from eqn.1b plus derivatives, is important for visualization, transparency, and credibility of the *regime ray*s, which reveal pathtimes/ pathlengths/ velocity detail, and thus quantifiable heterogeneity.

$$t_{O\,N} = t_{OE} = (\boldsymbol{r}_E \bullet \boldsymbol{n}_N)/\ v_N\,(\boldsymbol{n}_N,\ c_{i\,j}, \rho) = (x \sin\theta\cos\phi + y\sin\theta\sin\phi + z\cos\theta)/\ v_N\,(\theta, \phi\,;\, c_{i\,j}, \rho) \qquad (1a, 1b)$$

$$\begin{pmatrix} \frac{x}{t} \\ \frac{y}{t} \\ \frac{z}{t} \end{pmatrix} = \begin{pmatrix} n_x \\ n_y \\ n_z \end{pmatrix} * v_N + \begin{pmatrix} 1-n_x^2 & -n_x n_y & -n_x n_z \\ -n_x n_y & 1-n_y^2 & -n_y n_z \\ -n_x n_z & -n_y n_z & 1-n_z^2 \end{pmatrix} \begin{pmatrix} \frac{\partial v_N}{\partial n_x} \\ \frac{\partial v_N}{\partial n_y} \\ \frac{\partial v_N}{\partial n_z} \end{pmatrix} \ ; \quad \boldsymbol{n}_N = [\ n_x\ \ n_y\ \ n_z\ ] \qquad (2)$$

$$\left(\frac{x}{t}\right)^2 + \left(\frac{y}{t}\right)^2 + \left(\frac{z}{t}\right)^2 = v_E^{\ 2} = v_N^{\ 2} + \left(\frac{\partial v_N}{\partial\theta}\right)^2 + \left(\frac{1}{\sin\theta}\frac{\partial v_N}{\partial\phi}\right)^2 = v_N^{\ 2} + \left(\sqrt{\left(\frac{\partial v_N}{\partial\theta}\right)^2 + \left(\frac{1}{\sin\theta}\frac{\partial v_N}{\partial\phi}\right)^2}\right)^2 \qquad (3)$$

Six *regime rays* are simulated for qP-, qSV- and qSH-modes, from origin to cross-diagonal between [*x y z*] = [3 0 0] → [0 3 3], for equi-angle stepped front-normals. This sampling shows changes from near-surface in-layers-dominant to deeper cross-layers and at-slant-encountered cracks. The displays are km-spatial, with progression SPEEDS made tangible through dot-density [40 intervals per second]; <u>DENSE</u> is <u>slow</u> and <u>SPARSE</u> is <u>fast</u>! The action per se is virtually on the <u>energy flux loci</u> from **O**rigin to **E** shown in <u>RED</u>, but detail is visualized through *regime ray* segments; fine-dots <u>red</u> link the **E**-points. Front-normal **N**-points and dotted <u>*regime rays*</u> are <u>BLUE</u>; fine-dots-<u>blue</u> link the **N**-points. The <u>GREEN</u>-framed **R**-**E**-**N** triangles are tangent plane portions anchored at **E**, with pythagoras **R**ight angle <u>points linking to 2nd segments extended</u>.

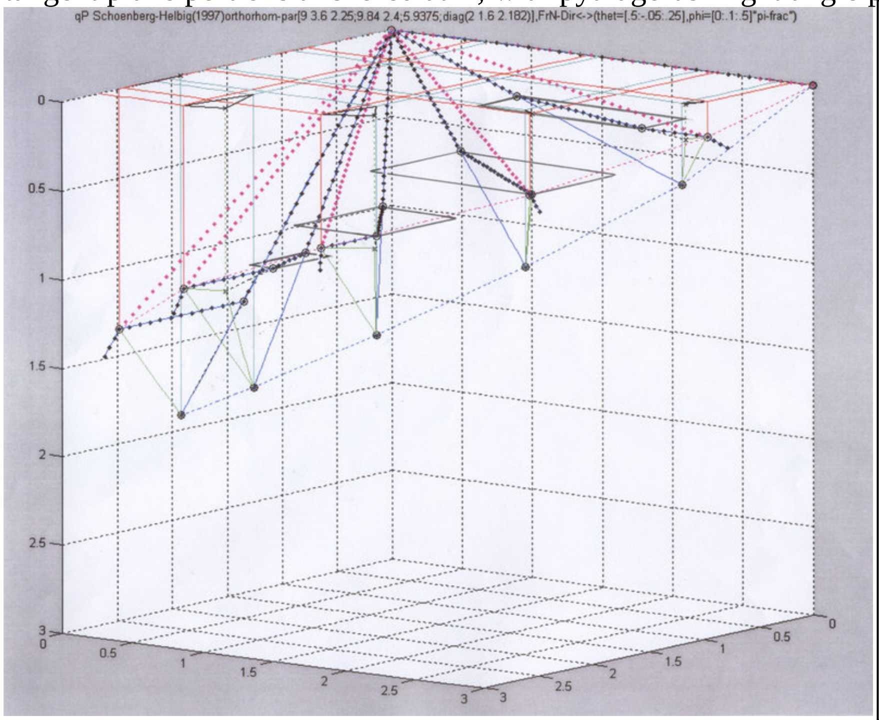

Fig.1: qP-mode *REGIME RAYS*
Schoenberg-Helbig orthorhrombic model
<u>Data for # 2 & # 4 ***FS-rays***</u>

2 directions *time length velo*
<u>E[. 9627 . 2619 . 0674] 1. 000 2. 9670 2. 9670</u>
N[. 9393 . 3052 . 1564] .4328 1..2775 2. 9516
Z[. 9511 . 3090 0] .4192 1. 2526 2. 9884
x[1. 0000 0 0] . 1480 . 4652 3. 1422
vTA=2. 9953 vRMS=2. 9959 vPM=2. 9966
lenPATH=2. 9953 vN=2. 9516
P[. 9574 . 2757 . 0860] Polarization ________

4 directions *time length velo*
<u>E[. 4817 . 5837 . 1577] 1. 000 2. 9101 2. 9101</u>
N[. 5237 . 7208 . 4540] . 5832 1. 6514 2. 8316
Z[. 5878 . 8090 0] . 2874 . 9133 3. 1780
y[0 1.0000 0] . 1294 . 5083 3. 9282
vTA=3. 0730 vRMS=3.0944 vPM=3. 1159
lenPATH=3. 0730 vN=2. 8316
P[. 5010 . 8097 . 3056] Polarization ________

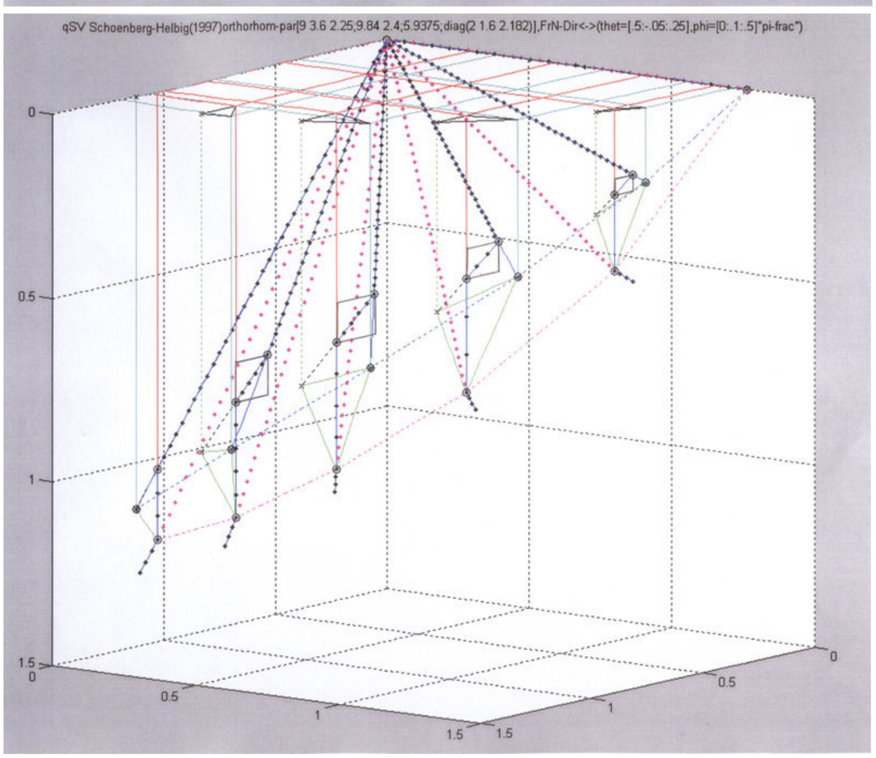

Fig.2: qSV-mode *REGIME RAYS*
Schoenberg-Helbig orthorhrombic model
<u>Data for # 2 & # 4 ***FS-rays***</u>

2 directions *time length velo*
<u>E[. 8757 . 3485 . 3342] 1. 000 1. 3243 1. 3243</u>
N[. 9393 . 3052 . 1564] . 9501 1..2346 1. 2995
X[0 . 3053 . 1564] . 0251 . 0952 3. 7889
z[0 0 1. 000] . 0248 . 2061 8. 3067
vTA=1. 5359 vRMS=1. 9175 vPM=2. 3939
lenPATH=1.5359 vN=1. 2995
P[-. 0652 -. 0838 . 9943] Polarization________

4 directions *time length velo*
<u>E[. 3946 . 6566 . 6427] 1. 000 1. 5100 1. 5100</u>
N[. 5237 . 7208 . 4540] . 7753 1. 1377 1. 4674
X[0 . 8462 . 5329] . 1176 . 2025 1. 7225
z[0 0 1.0000] . 1071 . 3460 3. 2322
vTA=1. 6863 vRMS=1.7711 vPM=1. 8602
lenPATH=1. 6863 vN=1. 4674
P[-. 2033 -. 2331 . 9510] Polarization _______

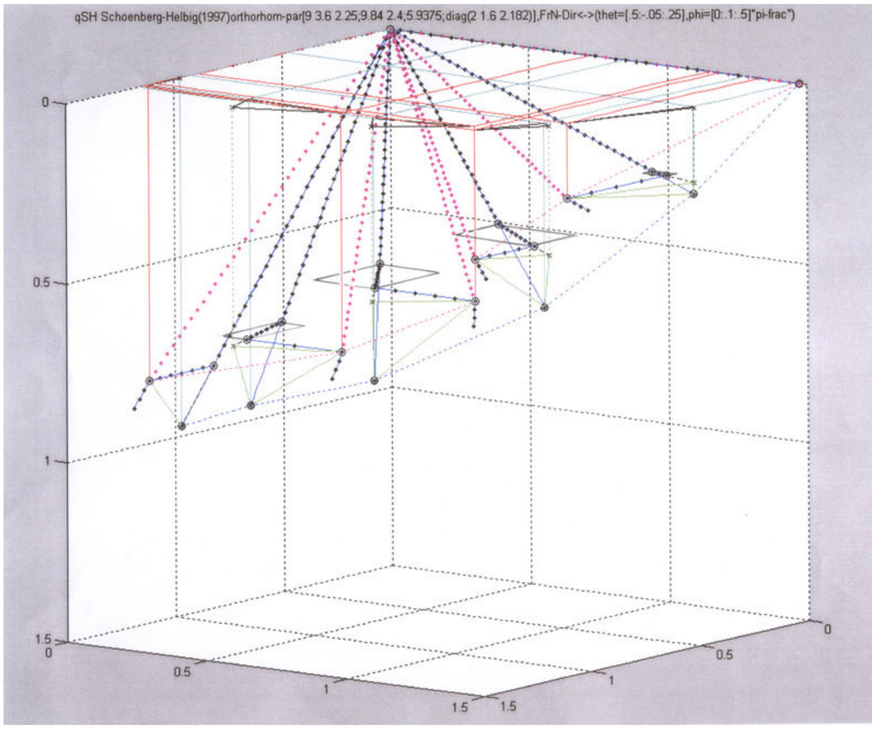

Fig.3: qSH-mode *REGIME RAYS*
Schoenberg-Helbig orthorhrombic model
Data for # 2 & # 4 ***FS-rays***

# 2 directions	*time*	*length*	*velo*
E[. 8236 . 5520 . 1302]	1. 000	1. 6154	1. 6154
N[. 9393 . 3052 . 1564]	. 8647	1..3445	1. 5548
Z[. 9511 . 3090 0]	..0451	. 0711	1. 5742
y[0 1.0000 0]	. 0902	. 4595	5. 0942

vTA=1. 8749 vRMS=2. 1314 vPM=2. 4229
lenPATH=1. 8749 vN=1. 5548
P[-. 2814 . 9576 . 0623] Polarization________

# 4 directions	*time*	*length*	*velo*
E[. 6945 . 6568 . .2938]	1. 000	1. 6571	1. 6571
N[. 5237 . 7208 . 4540]	. 6668	1. 0724	1. 6083
Z[. 5878 . 8090 0]	. 2160	. 3898	1. 8050
x[1.0000 0 0]	. 1172	. 3601	3. 0709

vTA=1. 8222 vRMS=1.8799 vPM=1. 9393
lenPATH=1. 8222 vN=1. 6083
P[-. 8412 . 5386 -. 0479] Polarization________

Focus initially on Fig.3 qSH-mode with its #2 *regime ray* and the boxed data. E-rowed underlined data is for red-dotted energy flux locus, so-called *group*- or *ray*-(velocity) representation. {N Z y} is code for regime ray segment orientations, here N for 3D front-normal, Z for in parallel to coordinate frame z-plane, and y for y-axis parallel. Segment 2 looks like a blur, but details the boundary of small z-plane rectangle with segment progressing diagonally; c.f. outlined plane areas for second segments of other *regime rays*. Note regime changed to {N Z x} for #4 *regime ray*, which through nearness of #3 and #4 energy flux loci suggests a 'flip-point', possibly even a cusping-like swerving. Attentive readers will notice and ponder the distinctly different *regime rays* patterns for the different modes; e.g. shear-modes *horizontal*/ *vertical* have second and third *regime ray* segments so-oriented. And remarkably FAST can manifest for third segments!

Conclusions

Regime rays encapsulate and quantify the fine structured anisotropic medium heterogeneity encountered along wave disturbance energy-transport channels through their significant direction and propagation speed detail. Because that detail links to parameters of relevant elastic medium models, they will be important for seismic wave propagation-, and particularly for anisotropy velocity field- modeling, as also potentially for data to-medium-models inversing. I expect *regime rays* will bring anisotropy kinematics back into the *FS-ray theory* purview, however with minor refinement of its premises.

References

Auld, B. A., 1973, Acoustic Fields and Waves in Solids, vol. I: John Wiley and Sons.

Cerveny, V. 2001, Seismic Ray Theory: Cambridge University Press.

Helbig, K., 1994, Foundations of Anisotropy for Exploration Seismics: Pergamon

Love, A.E.H., 1927, A Treatise on the Mathematical Theory of Elasticity: (1944 Dover republ. of 4th ed. Cambridge U. Press)

Macbeth, C., 2002, Multi-Component VSP Analysis for Applied Seismic Anisotropy: Pergamon.

Mensch, T., Rasolofosaon, P., 1997, Elastic-wave velocities in anisotropic media …: Geophysics Journal Internat, **128**, 43-64.

Rudzki, M.P., 1911, Parametrische Darstellung der elastischen Wellen in anisotropen Medien, Bulletin Academie Cracovie 503-536 (Parametric representation of elastic waves in anisotropic media).

Schoenberg, M., Helbig, K., 1997, Orthorhombic media: Modeling elastic wave behavior in … Geophysics, **62**, 1954-1974.

Vetter, W. J., 1993, The Fermat path … in anisotropic media: 63rd Annual Intern. Meeting, SEG, Expanded Abstract, 953-956.

Vetter, W. J., 2007, Anisotropy Kinematics Clarified though Regime Rays Model: 2007 CSPG CSEG Convention, 563-567.